IEEE Access
Multidisciplinary ⋮ Rapid Review ⋮ Open Access Journal

Received August 14, 2018, accepted September 7, 2018, date of publication September 17, 2018, date of current version October 8, 2018.

Digital Object Identifier 10.1109/ACCESS.2018.2870278

Blind Carrier Frequency Offset Estimation for MIMO-OFDM Systems Based on the Banded Structure of Covariance Matrices for Constant Modulus Signals

LIU YANG[1], (Student Member, IEEE), HANG ZHANG[1], (Member, IEEE), YANG CAI[2], AND HUA YANG[1], (Student Member, IEEE)

[1]College of Communications Engineering, Army Engineering University of PLA, Nanjing 210007, China
[2]Department of Electric and Optical Engineering, Space Engineering University of PLA, Beijing 101416, China

Corresponding author: Liu Yang (yl755551@163.com)

This work was supported by the Natural Science Foundation of China under Grant 61671475.

ABSTRACT This paper addresses the problem of blind carrier frequency offset (CFO) estimation for multi-input-multi-output orthogonal frequency division multiplexing systems. Benefiting from the banded structure of the circulant channel matrix from each transmitting antenna to each receiving antenna, the covariance matrices formulated by circular shifts of received signals also possess the banded structure in the absence of CFO for constant modulus signals. Thus, the cost function can be constructed by minimizing the elements outside the band and a closed-form CFO estimation algorithm is proposed. Since the channel length has an effect on the proposed estimator and channels with high delay spreads may deteriorate the estimation performance, an improved version of the proposed algorithm is investigated under the assumption that the channel remains constant within two consecutive OFDM symbols which is often the case. Experimental results demonstrate that the proposed algorithm shows better performance than the conventional CFO estimation schemes in frequency-selective fading channels and the improved version of the proposed algorithm can further optimize the estimation performance under long channel length conditions.

INDEX TERMS Blind estimation, banded structure, carrier frequency offset (CFO), multi-input multi-output orthogonal frequency division multiplexing (MIMO-OFDM).

I. INTRODUCTION

Orthogonal frequency division multiplexing (OFDM) has been the most promising multicarrier modulation technique during the past two decades due to its high bandwidth efficiency and immunity against multipath propagation. It has been adopted by many wireless standards and applications such as IEEE 802.11, fourth generation long term evolution (4G LTE) [1] and some wired applications like digital audio and video broadcasting. Besides, OFDM is a strong candidate for the forthcoming fifth generation (5G) wireless communication together with the multi-input multi-output (MIMO) technology [2]. The combination of the two major techniques can greatly improve the system capacity to meet the increasing demand for very high data rates. However, OFDM is quite sensitive to carrier frequency offset (CFO) resulted from the mismatch between transceivers or Doppler frequency shift. The CFO problem persists in MIMO-OFDM systems and results in inter-carrier interference (ICI) that can cause serious performance degradation.

Various CFO estimation schemes have been developed during the past few years and they can be categorized as data-aided ones and semi-blind/ blind ones. The semi-blind or blind algorithms are attractive due to the high bandwidth efficiency. In [3], a subspace based semi-blind algorithm is proposed for joint CFO and channel estimation, despite using one pilot OFDM block, hundreds of data blocks are required to achieve satisfied estimation performance which is not appropriate for fast time-varying channels. Besides, the number of receiving antennas is required to be larger than that of transmitting antennas. Similarly, another example by exploiting the multi-antenna redundancy at the receiver is the work in [4], which requires the number of receiving antennas to be at least one more than that of the transmitting antennas. A blind CFO estimation algorithm based on tensor decomposition is developed in [5] and [6], however, it is only suitable for single-input multi-output (SIMO) OFDM systems and the number of data blocks should be no less than the number of subcarriers. In [7], a kurtosis-type criterion is exploited for CFO estimation in SISO and MIMO-OFDM systems, but the estimation performance is poor under highly frequency-selective channels. The work in [8] develops a blind CFO estimator by minimizing the components of the signal power spectrum, but the performance is poor under long channel length conditions. The algorithms in [9] and [10] assume that the channel frequency response is almost the same on two neighboring subcarriers, thus by minimizing the power difference between two adjacent subcarriers with constant modulus (CM) signaling, the CFO can be estimated. In [11] and [12], the algorithms utilize the information in time domain and construct the cost function by minimizing the power difference between two adjacent OFDM symbols under the assumption that the channel changes slowly over two successive OFDM symbols. A more robust algorithm exploiting the banded structure of the covariance matrix calculated by circular shifts of the received signal is proposed in [13]–[14] and CFO estimation with higher accuracy is obtained. The algorithm in [15] further improves the algorithm in [14] by incorporating the time domain information to alleviate the performance loss brought about by long channel length. Nevertheless, the algorithms in [9]– [15] are designed for SISO-OFDM systems. The work in [16] proposes a frequency synchronization scheme for multiuser uplink OFDM systems by exploiting the angle information of users, but the assumption that perfect knowledge about angular spread is available at the BS is not practical. The algorithm in [17] develops a CFO estimator via rank reduction criterion, but the number of OFDM symbols in one data block should be no less than three when there are two receiving antennas and when the number of receiving antennas grows, the data block is required to be larger.

In this paper, a new CFO estimation algorithm is proposed for MIMO-OFDM systems. On one hand, the number of receiving antennas is not required to be larger than that of the transmitting antennas; On the other hand, the proposed estimator can work in the case when there is only one OFDM symbol in a data block. The proposed method is based on the banded structure of auto-covariance and cross-covariance matrices calculated by circular shifts of multiple received signals. By minimizing the out-of-band elements of covariance matrices, a closed form estimator is constructed and a simple curve fitting method can be employed to find the minimum of the contrast function. In order to mitigate the performance degradation caused by long channel length, the proposed algorithm is further optimized by utilizing the in-band elements of covariance matrices. Performance of the proposed algorithms is analyzed and compared with other schemes under frequency-selective fading channels.

The rest of the paper is organized as follows. The MIMO-OFDM system model in the presence of CFO is introduced in Section II. Section III shows the proposed CFO estimation algorithm and its improved version. The Cramer-Rao lower bound (CRLB) of CFO estimation for MIMO-OFDM systems is derived in Section IV. The experimental results and analysis are given in Section V and Section VI includes some concluding remarks.

Notations: Throughout the work, the notation $|\cdot|$ refers to the complex modulus and $\|\cdot\|$ stands for the matrix Frobenius norm. The real and imaginary part of $\mathbf{a} \in \mathbb{C}^{N\times 1}$ are denoted by $Re\{\mathbf{a}\}$ and $Im\{\mathbf{a}\}$, respectively, and $diag\{\mathbf{a}\} \in \mathbb{C}^{N\times N}$ denotes the diagonal matrix holding the elements of $\mathbf{a}$ on its diagonal. The identity matrix is denoted by $\mathbf{I}_N \in \mathbb{C}^{N\times N}$ and the all-ones vector is denoted by $\mathbf{1}_N = [1, \ldots, 1]^T \in \mathbb{C}^N$. The superscripts $(\cdot)^H$, $(\cdot)^T$ and $(\cdot)^*$ denote the Hermitian transpose, transpose and complex conjugate operator, respectively.

II. SYSTEM MODEL AND PROBLEM FORMULATION

Consider a point-to-point MIMO-OFDM system with N_T transmitting antennas, N_R receiving antennas and N subcarriers as shown in Fig. 1. The frequency-selective channel with length L is block fading and the channel state information (CSI) remains constant among N_S OFDM symbols. Let $\mathbf{S}_k(i) = [S_k^0(i), S_k^1(i), \ldots, S_k^{N-1}(i)]^T$ denote the i-th ($i = 1, 2, \ldots, N_S$) data symbol transmitted by the k-th ($k = 1, 2, \ldots, N_T$) transmitting antenna, the element is assumed to be constant modulus with $\left|S_k^n(i)\right|^2 = 1, n = 0, 1, \ldots, N-1$. The signal is firstly transformed to time domain by an N point IDFT and prepended with a cyclic prefix (CP) consists of the copy of the last L_{CP} ($L_{CP} \geq L$) entries of each OFDM symbol. The OFDM symbols are then transmitted through a multipath channel. Denote ε as the CFO between the transmitter and the receiver, normalized by subcarrier spacing, then ε is in the range of $(-0.5, 0.5)$ [18]. At each receiver, after removing the CP, the time domain signal received by the m-th receiving antenna can be expressed by

$$\mathbf{x}_m(i) = \varphi^{(\varepsilon)}(i) \sum_{k=1}^{N_T} \Theta(\varepsilon)\Phi_{m,k}\mathbf{F}^H\mathbf{S}_k(i) + \mathbf{z}_m(i), \quad m = 1, 2, \ldots, N_R \tag{1}$$

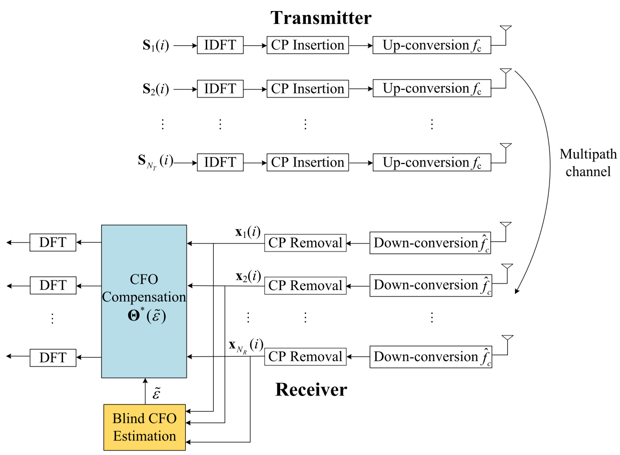

FIGURE 1. System model for a point to point MIMO-OFDM system with a blind CFO estimation module.

where $\varphi^{(\varepsilon)}(i) = e^{j2\pi i\varepsilon(N+L_{CP})/N}$ is the common phase shift of the i-th OFDM symbol and $\Theta(\varepsilon)$ is the diagonal CFO matrix denoted by

$$\Theta(\varepsilon) = diag\{[1, e^{j2\pi\varepsilon/N}, \ldots, e^{j2\pi(N-1)\varepsilon/N}]\} \tag{2}$$

$\mathbf{F}$ is the $N \times N$ DFT matrix with its entry (u, v) given by $\mathbf{F}(u, v) = 1/\sqrt{N}e^{-j2\pi uv/N}$, $(u, v = 0, 1, \ldots, N-1)$ and $\mathbf{z}_m(i)$ is the additive white Gaussian noise (AWGN) vector. Affected by CP appending and removing, the channel matrix $\Phi_{m,k}$ is a circular convolution matrix, which can be written as

$$\Phi_{m,k} = \begin{bmatrix} h^0_{m,k} & h^{N-1}_{m,k} & \cdots & h^1_{m,k} \\ h^1_{m,k} & h^0_{m,k} & \cdots & h^2_{m,k} \\ \vdots & \vdots & \ddots & \vdots \\ h^{N-1}_{m,k} & h^{N-2}_{m,k} & \cdots & h^0_{m,k} \end{bmatrix} \tag{3}$$

in which $\mathbf{h}_{m,k} = [h^0_{m,k}, h^1_{m,k}, \ldots, h^{L-1}_{m,k}, \ldots, h^{N-1}_{m,k}]^T$ is the channel impulse response vector from the k-th transmitter to the m-th receiver and $h^l_{m,k} = 0$ for $l \geq L$. An appealing nature of the circulant channel matrix is that it can be diagonalized by the DFT matrix, i. e. $\Phi_{m,k} = \mathbf{F}^H \Lambda \mathbf{F}$ and Λ is a diagonal matrix.

According to (1), since $\mathbf{F}\Theta(\varepsilon)\mathbf{F}^H \neq \mathbf{I}$ ($\mathbf{I}$ is an identity matrix), the orthogonality between subcarriers is destroyed by the CFO and ICI is produced. Hence the CFO must be compensated before DFT implementation. The purpose of this work is to get the compensation matrix $\Theta^*(\tilde{\varepsilon})$ formed by the estimated CFO $\tilde{\varepsilon}$ from the receiving signals in the absence of CSI and without using training sequences.

III. PROPOSED CFO ESTIMATION ALGORITHMS FOR MIMO-OFDM SYSTEMS

A. PROPOSED CFO ESTIMATION ALGORITHM

Let $\hat{\varepsilon}$ denote the trial value of CFO and the compensated CFO matrix is represented by $\Theta^*(\hat{\varepsilon})$, i. e. the complex conjugate of $\Theta(\hat{\varepsilon})$. Then the corrected received signals can be expressed by

$$\mathbf{y}_{m,\hat{\varepsilon}}(i) = \varphi^{(\varepsilon-\hat{\varepsilon})}(i) \sum_{k=1}^{N_T} \Theta(\varepsilon - \hat{\varepsilon})\Phi_{m,k}\mathbf{F}^H\mathbf{S}_k(i) + \Theta^*(\hat{\varepsilon})\mathbf{z}_m(i), \quad m = 1, 2, \ldots, N_R \tag{4}$$

A matrix can be formed by stacking circularly shifted column vectors, i. e.

$$\begin{aligned} \mathbf{D}_{m,\hat{\varepsilon}}(i) &= [\mathbf{y}_{m,\hat{\varepsilon}}(i), \mathbf{P}\mathbf{y}_{m,\hat{\varepsilon}}(i), \ldots, \mathbf{P}^{N-1}\mathbf{y}_{m,\hat{\varepsilon}}(i)] \\ &= \begin{bmatrix} y^0_{m,\hat{\varepsilon}}(i) & y^1_{m,\hat{\varepsilon}}(i) & \cdots & y^{N-2}_{m,\hat{\varepsilon}}(i) & y^{N-1}_{m,\hat{\varepsilon}}(i) \\ y^1_{m,\hat{\varepsilon}}(i) & y^2_{m,\hat{\varepsilon}}(i) & \cdots & y^{N-1}_{m,\hat{\varepsilon}}(i) & y^0_{m,\hat{\varepsilon}}(i) \\ \vdots & \vdots & \ddots & \vdots & \vdots \\ y^{N-2}_{m,\hat{\varepsilon}}(i) & y^{N-1}_{m,\hat{\varepsilon}}(i) & \cdots & y^{N-4}_{m,\hat{\varepsilon}}(i) & y^{N-3}_{m,\hat{\varepsilon}}(i) \\ y^{N-1}_{m,\hat{\varepsilon}}(i) & y^0_{m,\hat{\varepsilon}}(i) & \cdots & y^{N-3}_{m,\hat{\varepsilon}}(i) & y^{N-2}_{m,\hat{\varepsilon}}(i) \end{bmatrix} \end{aligned} \tag{5}$$

in which $\mathbf{P}^n$ $(n = 0, 1, \ldots, N-1)$ are permutation matrices. The covariance matrix between the m_1-th received signal and the m_2-th received signal can be obtained from (5) as

$$\mathbf{R}_{m_1,m_2,\hat{\varepsilon}}(i) = \frac{1}{N}\mathbf{D}_{m_1,\hat{\varepsilon}}(i)\mathbf{D}^H_{m_2,\hat{\varepsilon}}(i) \tag{6}$$

Assuming that the CFO is perfectly estimated, the above covariance matrix can be expressed by

$$\begin{aligned} \mathbf{R}_{m_1,m_2}(i) &= \frac{1}{N}\sum_{n=0}^{N-1} \mathbf{P}^n \mathbf{y}_{m_1}(i)\mathbf{y}^H_{m_2}(i)(\mathbf{P}^n)^H \\ &= \frac{1}{N}\sum_{n=0}^{N-1} \mathbf{P}^n(\sum_{k_1=1}^{N_T} \Phi_{m_1,k_1}\mathbf{F}^H\mathbf{S}_{k_1}(i) + \mathbf{z}_{m_1}(i)) \\ &\quad \cdot (\sum_{k_2=1}^{N_T} \Phi_{m_2,k_2}\mathbf{F}^H\mathbf{S}_{k_2}(i) + \mathbf{z}_{m_2}(i))^H(\mathbf{P}^n)^H \end{aligned} \tag{7}$$

Due to the circulant property of permutation matrices and the channel matrix, (7) can be rewritten as

$$\begin{aligned} \mathbf{R}_{m_1,m_2}(i) &= \frac{1}{N}\sum_{k_1=1}^{N_T}\sum_{k_2=1}^{N_T} \Phi_{m_1,k_1} \\ &\quad \cdot \underbrace{\sum_{n=0}^{N-1} \mathbf{P}^n\mathbf{F}^H\mathbf{S}_{k_1}(i)\mathbf{S}^H_{k_2}(i)\mathbf{F}(\mathbf{P}^n)^H}_{\mathbf{T}} \cdot \Phi^H_{m_2,k_2} + \mathbf{e} \end{aligned} \tag{8}$$

in which $\mathbf{e}$ is the total error matrix generated by noise. When $k_1 = k_2$, the (p, q)-th element t_{pq} of matrix $\mathbf{T}$ is

$$\begin{aligned} t_{pq} &= \sum_{n=0}^{N-1}\sum_{l_1=0}^{N-1} S^{l_1}_{k_1}(i)e^{j\frac{2\pi l_1 n}{N}} \sum_{l_2=0}^{N-1} S^{l_2}_{k_1}{}^*(i)e^{-j\frac{2\pi l_2(n+p-q)}{N}} \\ &= \sum_{l=0}^{N-1} S^l_{k_1}(i) \cdot S^l_{k_1}{}^*(i)e^{-j\frac{2\pi l(p-q)}{N}} \\ &= \begin{cases} N, & p = q \\ 0, & p \neq q \end{cases} \end{aligned} \tag{9}$$

which indicates that $\mathbf{T}$ is a diagonal matrix and $\mathbf{T}$ is no longer diagonal when $k_1 \neq k_2$. In this case, $\mathbf{R}_{m_1,m_2}(i)$ can be split into two parts and expressed by

$$\begin{aligned} \mathbf{R}_{m_1,m_2}(i) &= \sum_{k=1}^{N_T} \Phi_{m_1,k}\Phi^H_{m_2,k} \\ &\quad + \frac{1}{N}\sum_{k_1=1}^{N_T}\sum_{\substack{k_2=1 \\ k_2\neq k_1}}^{N_T} \Phi_{m_1,k_1}\mathbf{A}_{k_1,k_2}\Phi^H_{m_2,k_2} + \mathbf{e} \end{aligned} \tag{10}$$

in which $\mathbf{A}_{k_1,k_2} = \sum_{n=0}^{N-1} \mathbf{P}^n\mathbf{F}^H\mathbf{S}_{k_1}(i)\,\mathbf{S}^H_{k_2}(i)\mathbf{F}(\mathbf{P}^n)^H$ is a non-diagonal matrix. Since $\Phi_{m,k}$ in (3) has banded structure, it can be easily obtained that the banded structure maintains in $\sum_{k=1}^{N_T} \Phi_{m_1,k}\Phi^H_{m_2,k}$. Denote $\mathbf{r}_{m_1,m_2}(i) = [r^0_{m_1,m_2}(i), r^1_{m_1,m_2}(i), \ldots, r^{N-1}_{m_1,m_2}(i)]^T$ as the first column of

$\sum_{k=1}^{N_T} \Phi_{m_1,k}\Phi_{m_2,k}^H$, there is

$$\left|r_{m_1,m_2}^n(i)\right|^2 \begin{cases} > 0, & 0 \le n \le L-1 \\ = 0, & L \le n \le N-L \\ > 0, & N-L+1 \le n \le N-1 \end{cases} \tag{11}$$

which indicates that some components of $\mathbf{r}_{m_1,m_2}(i)$ are missing/out of band at some specific positions. Although the existence of the second term of (10) weakens the banded structure of $\mathbf{R}_{m_1,m_2}(i)$, it should be noted that if CFO is not estimated correctly, the banded nature will be further weakened. Therefore, the weakened banded structure of $\mathbf{R}_{m_1,m_2}(i)$ can be utilized for CFO estimation. In the following analysis, we assume that $\mathbf{R}_{m_1,m_2}(i) \approx \sum_{k=1}^{N_T} \Phi_{m_1,k}\Phi_{m_2,k}^H + \mathbf{e}$ for simple derivation. Since $\mathbf{R}_{m_1,m_2,\hat{\varepsilon}}(i)$ is Toeplitz, the first column of $\mathbf{R}_{m_1,m_2,\hat{\varepsilon}}(i)$ is sufficient and it can be calculated by

$$\mathbf{r}_{m_1,m_2,\hat{\varepsilon}}(i) = \frac{1}{N}\mathbf{D}_{m_1,\hat{\varepsilon}}(i)\mathbf{y}_{m_2,\hat{\varepsilon}}^*(i) \tag{12}$$

Thus the cost function can be achieved by minimizing the out-of-band elements of $\mathbf{r}_{m_1,m_2,\hat{\varepsilon}}(i)$, i. e.

$$\begin{aligned} J(\hat{\varepsilon}) &= \sum_{i=1}^{N_S}\sum_{m_1=1}^{N_R}\sum_{m_2=m_1}^{N_R}\sum_{n=L}^{N-L}\left|r_{m_1,m_2,\hat{\varepsilon}}^n(i)\right|^2 \\ \tilde{\varepsilon} &= \arg\min_{\hat{\varepsilon}} J(\hat{\varepsilon}) \end{aligned} \tag{13}$$

Following a procedure similar to the one described in [7], the cost function $J(\hat{\varepsilon})$ can be approximated by a closed form function (see Appendix **A**)

$$J(\hat{\varepsilon}) \approx Acos(2\pi(\varepsilon - \hat{\varepsilon})) - A \tag{14}$$

in which A is a constant irrelevant with ε and $\hat{\varepsilon}$. Since $A < 0$, the function $J(\hat{\varepsilon})$ reaches the minimum when $\hat{\varepsilon} = \varepsilon$. The function in (14) follows a sinusoidal structure, hence the minimization process can be performed by a curve-fitting method instead of exhaustive line search. Specifically, the value of $J(\hat{\varepsilon})$ is calculated at three points $\hat{\varepsilon} = \frac{1}{4}, -\frac{1}{4}, 0$ and the estimation of ε can be obtained by

$$\tilde{\varepsilon} = \begin{cases} \frac{1}{2\pi}\tan^{-1}(\frac{b}{a}), & a \ge 0 \\ \frac{1}{2\pi}\tan^{-1}(\frac{b}{a}) - \frac{1}{2}, & a < 0,\ b > 0 \\ \frac{1}{2\pi}\tan^{-1}(\frac{b}{a}) + \frac{1}{2}, & a < 0,\ b \le 0 \end{cases} \tag{15}$$

where $a = (J(1/4)+J(-1/4))/2-J(0)$ and $b = (J(-1/4)-J(1/4))/2$.

B. AN IMPROVED VERSION OF THE PROPOSED CFO ESTIMATION ALGORITHM

It can be observed from (13) that the number of the out-of-band elements depends on the channel length L when the number of subcarriers N is fixed, and channels with high delay spreads may deteriorate the CFO estimation performance. The drawback can be compensated by combining the in-band information under the assumption that the channel effect remains constant between two consecutive OFDM symbols. Specifically, $\mathbf{r}_{m_1,m_2,\hat{\varepsilon}}(i)$ can be re-expressed by

$$\begin{aligned} \mathbf{r}_{m_1,m_2,\hat{\varepsilon}}(i) = [&r_{m_1,m_2,\hat{\varepsilon}}^0(i), \ldots, r_{m_1,m_2,\hat{\varepsilon}}^{L-1}(i), \tilde{r}_{m_1,m_2,\hat{\varepsilon}}^L(i), \ldots, \\ &\tilde{r}_{m_1,m_2,\hat{\varepsilon}}^{N-L}(i), r_{m_1,m_2,\hat{\varepsilon}}^{N-L+1}(i), \ldots, r_{m_1,m_2,\hat{\varepsilon}}^{N-1}(i)]^T \end{aligned} \tag{16}$$

where $\mathbf{r}_{m_1,m_2,\hat{\varepsilon}}(i)$ is split into two parts, i. e. the in-band vector $\mathbf{r}_{m_1,m_2,\hat{\varepsilon}}^{\text{NZ}}(i)$ and the out-of-band vector $\mathbf{r}_{m_1,m_2,\hat{\varepsilon}}^{\text{Z}}(i)$ which are defined as $\mathbf{r}_{m_1,m_2,\hat{\varepsilon}}^{\text{NZ}}(i) = [r_{m_1,m_2,\hat{\varepsilon}}^0(i), \ldots, r_{m_1,m_2,\hat{\varepsilon}}^{L-1}(i), r_{m_1,m_2,\hat{\varepsilon}}^{N-L+1}(i), \ldots, r_{m_1,m_2,\hat{\varepsilon}}^{N-1}(i)]^T$ and $\mathbf{r}_{m_1,m_2,\hat{\varepsilon}}^{\text{Z}}(i) = [\tilde{r}_{m_1,m_2,\hat{\varepsilon}}^L(i), \ldots, \tilde{r}_{m_1,m_2,\hat{\varepsilon}}^{N-L}(i)]^T$, respectively. Now the improved cost function can be formulated as

$$\begin{aligned} J^I(\hat{\varepsilon}) = &\sum_{i=1}^{N_S-1}\sum_{m_1=1}^{N_R}\sum_{m_2=m_1}^{N_R}\{(\left\|\mathbf{r}_{m_1,m_2,\hat{\varepsilon}}^{\text{NZ}}(i+1) - \mathbf{r}_{m_1,m_2,\hat{\varepsilon}}^{\text{NZ}}(i)\right\|^2) \\ &+ (\left\|\mathbf{r}_{m_1,m_2,\hat{\varepsilon}}^{\text{Z}}(i+1)\right\|^2 + \left\|\mathbf{r}_{m_1,m_2,\hat{\varepsilon}}^{\text{Z}}(i)\right\|^2)\} \\ \tilde{\varepsilon} = &\arg\min_{\hat{\varepsilon}} J^I(\hat{\varepsilon}) \end{aligned} \tag{17}$$

The above cost function incorporates both the out-of-band and in-band information, hence the performance loss brought by long channel response can be compensated by the first term in (17). The improved cost function can be approximated as (see Appendix **B**)

$$J^I(\hat{\varepsilon}) \approx Bcos(2\pi(\varepsilon - \hat{\varepsilon})) - B \tag{18}$$

in which $B < 0$ is a constant independent of ε and $\hat{\varepsilon}$.

C. COMPUTATIONAL COMPLEXITY ANALYSIS

In this section, the computational complexities of the proposed algorithms and the compared algorithms are evaluated in terms of complex multiplications. The state of art algorithms in [7], [9], [11], [13], and [15] are labelled as "Kurtosis", "PDE-F", "PDE-T", "Cov" and "Cov-fitting", respectively. Although the cost functions in [11], [13], and [15] are designed for SISO-OFDM systems, they can be generalized to MIMO-OFDM systems by summating the cost function corresponding to each received signal just like the way in [7] and [9]. The numerical complexity of the proposed algorithm mainly comes from calculating the first column of the covariance matrices and calculating the square absolute value of the out-of-band elements. The number of covariance matrices is $\frac{1}{2}N_R(N_R+1)$, thus the first part and second part calculation require $\frac{1}{2}N_R(N_R+1) \times 3N^2 \times N_S$ and $\frac{1}{2}N_R(N_R+1) \times 3(N-2L+1) \times N_S$ multiplications, respectively. Similarly, the improved version of the proposed algorithm named "Proposed-fitting" requires extra calculation for the in-band elements, thus adding $\frac{1}{2}N_R(N_R+1) \times 3(2L-1) \times N_S$ multiplications compared with the proposed algorithm. For the "Cov" and "Cov-fitting" methods, the number of covariance matrices needed for calculation is N_R, which leads to less computational complexities compared with the proposed and "Proposed-fitting" methods.

TABLE 1. Computational complexities comparison.

Methods	Computational complexity
Proposed	$\frac{3}{2}N_R(N_R+1)(N^2+N-2L+1)N_S$
Proposed-fitting	$\frac{3}{2}N_R(N_R+1)(N^2+N)N_S$
Cov	$3N_R(N^2+N-2L+1)N_S$
Cov-fitting	$3N_R(N^2+N)N_S$
Kurtosis	$3N_RN(\log_2 N+3)N_S$
PDE-F	$3N_RN(\log_2 N+1)N_S$
PDE-T	$3N_RN(\log_2 N+1)N_S$

The "Kurtosis" algorithm requires $3N_RN_SN\log_2 N$ multiplications for DFT and $9N_RN_SN$ multiplications for kurtosis calculation. As for the "PDE-T" and "PDE-F" methods, they require $3N_RN_SN\log_2 N$ multiplications for DFT and $3N_RN_SN$ multiplications for the square absolute value calculation of the elements. In summary, the computational complexities of the mentioned algorithms are listed in Table 1. Since the number of subcarriers N is usually larger than that of the receiving antennas N_R, the proposed algorithms cost more than the compared algorithms.

IV. CRAMER-RAO LOWER BOUND

In this section, the CRLB of CFO estimation for MIMO-OFDM systems is derived. For the simplicity of expression, (1) is rewritten as

$$\mathbf{x}_m(i) = \Theta(\varepsilon)\mathbf{F}^H \sum_{k=1}^{N_T} diag\{\bar{\mathbf{S}}_k(i)\}\mathbf{H}_{m,k} + \mathbf{z}_m(i) \tag{19}$$

in which $\mathbf{H}_{m,k} = [H_{m,k}(1), H_{m,k}(2), \ldots, H_{m,k}(N)]^T \in \mathbb{C}^{N\times 1}$ is the frequency domain channel response and $diag\{\mathbf{H}_{m,k}\} = \mathbf{F}^H\Phi_{m,k}\mathbf{F}$. $\bar{\mathbf{S}}_k(i) = \varphi^{(\varepsilon)}(i)\mathbf{S}_k(i)$ denotes the equivalent transmitted symbol under the effect of accumulative phase shift. We place the vectors $\mathbf{x}_m(i), m = 1, 2, \ldots, N_R$ next to each other and obtain the following $N \times N_R$ matrices

$$\begin{aligned}\mathbf{X}(i) &= [\mathbf{x}_1(i), \mathbf{x}_2(i), \ldots, \mathbf{x}_{N_R}(i)]\\ &= \Theta(\varepsilon)\mathbf{F}^H \sum_{k=1}^{N_T} diag\{\bar{\mathbf{S}}_k(i)\}\mathbf{H}_k + \mathbf{Z}(i)\end{aligned} \tag{20}$$

in which $\mathbf{H}_k = [\mathbf{H}_{1,k}, \mathbf{H}_{2,k}, \ldots, \mathbf{H}_{N_R,k}] \in \mathbb{C}^{N\times N_R}$ and $\mathbf{Z}(i) = [\mathbf{z}_1(i), \mathbf{z}_2(i), \ldots, \mathbf{z}_{N_R}(i)] \in \mathbb{C}^{N\times N_R}$. Let $\odot$ and $\otimes$ denote the Khatri-Rao product and Kronecker product, respectively, by defining $\mathbf{V}^{(k)} = (\Theta(\varepsilon) \otimes \mathbf{I}_{N_R})(\mathbf{F}^* \odot \mathbf{H}_k^T)$, $\mathbf{V} = [\mathbf{V}^{(1)}, \mathbf{V}^{(2)}, \ldots, \mathbf{V}^{(N_T)}]$, and $\tilde{\mathbf{S}}(i) = [\bar{\mathbf{S}}_1^T(i), \bar{\mathbf{S}}_2^T(i), \ldots, \bar{\mathbf{S}}_{N_T}^T(i)]^T$, (20) can be rewritten as

$$vec(\mathbf{X}^T(i)) = \mathbf{V}\tilde{\mathbf{S}}(i) + vec(\mathbf{Z}^T(i)) \tag{21}$$

where $vec(\cdot)$ denotes the vectorization operator.

For constant modulus signals, $\tilde{\mathbf{S}}(i)$ can be denoted as $\tilde{\mathbf{S}}(i) = [e^{j\theta_{1,i}}, e^{j\theta_{2,i}}, \ldots, e^{j\theta_{N_TN,i}}]^T$, thus by denoting $\boldsymbol{\theta}(i) = [\theta_{1,i}, \theta_{2,i}, \ldots, \theta_{N_TN,i}]^T$ and $\mathbf{H} = [\mathbf{H}_1^T, \mathbf{H}_2^T, \ldots, \mathbf{H}_{N_T}^T]$, the unknown parameters can be expressed as $\alpha = [\boldsymbol{\theta}^T(1), \boldsymbol{\theta}^T(2), \ldots, \boldsymbol{\theta}^T(N_S), \varepsilon, Re\{vec(\mathbf{H})^T\}, Im\{vec(\mathbf{H})^T\}]^T$. Then the components of the Fisher information matrix can be given by

$$[\mathrm{CRLB}^{-1}\{\alpha\}]_{m,n} = \frac{2}{\sigma_z^2} Re\{\sum_{i=1}^{N_S}[\frac{\partial\mathbf{V}\tilde{\mathbf{S}}(i)}{\partial\alpha_m}]^H[\frac{\partial\mathbf{V}\tilde{\mathbf{S}}(i)}{\partial\alpha_n}]\} \tag{22}$$

where σ_z^2 is the noise variance and α_m is the m-th element of α. After some tedious yet straightforward calculations, the following matrix can be obtained

$$\Gamma = \begin{bmatrix}\Gamma_1 & \Gamma_2 & j\Gamma_2\\ \Gamma_2^H & \Gamma_3 & j\Gamma_3\\ -j\Gamma_2^H & -j\Gamma_3^H & \Gamma_3\end{bmatrix} \tag{23}$$

where

$$\begin{aligned}\Gamma_1 &= \sum_{i=1}^{N_S}[\frac{\partial\mathbf{V}\tilde{\mathbf{S}}(i)}{\partial\varepsilon}]^H[\frac{\partial\mathbf{V}\tilde{\mathbf{S}}(i)}{\partial\varepsilon}] = \sum_{i=1}^{N_S}\tilde{\mathbf{S}}^H(i)\mathbf{V}^H\mathbf{D}^H\mathbf{D}\mathbf{V}\tilde{\mathbf{S}}(i)\\ \Gamma_2 &= \sum_{i=1}^{N_S}[\frac{\partial\mathbf{V}\tilde{\mathbf{S}}(i)}{\partial\varepsilon}]^H[\frac{\partial\mathbf{V}\tilde{\mathbf{S}}(i)}{\partial vec(\mathbf{H})}]\\ &= \sum_{i=1}^{N_S}\tilde{\mathbf{S}}^H(i)\mathbf{V}^H D^H((\Theta(\varepsilon)(\mathbf{1}_{1\times N_T}\otimes\mathbf{F}^*)diag\{\tilde{\mathbf{S}}(i)\})\otimes\mathbf{I}_{N_R})\\ \Gamma_3 &= \sum_{i=1}^{N_S}[\frac{\partial\mathbf{V}\tilde{\mathbf{S}}(i)}{\partial vec(\mathbf{H})}]^H[\frac{\partial\mathbf{V}\tilde{\mathbf{S}}(i)}{\partial vec(\mathbf{H})}]\\ &= \sum_{i=1}^{N_S}(diag\{\tilde{\mathbf{S}}^*(i)\}(\mathbf{1}_{N_T\times N_T}\otimes\mathbf{I}_N)diag\{\tilde{\mathbf{S}}(i)\})\otimes\mathbf{I}_{N_R}\end{aligned} \tag{24}$$

in which $\mathbf{D} = j\frac{2\pi}{N}diag\{0, 1, \ldots, N-1\}\otimes\mathbf{I}_{N_R}$.

Define

$$\begin{aligned}\Xi_{1,i} &= [\frac{\partial\mathbf{V}\tilde{\mathbf{S}}(i)}{\partial\boldsymbol{\theta}(t)}]^H[\frac{\partial\mathbf{V}\tilde{\mathbf{S}}(i)}{\partial\varepsilon}] = -j\cdot diag\{\tilde{\mathbf{S}}^*(i)\}\mathbf{V}^H\mathbf{D}\mathbf{V}\tilde{\mathbf{S}}(i)\\ \Xi_{2,i} &= [\frac{\partial\mathbf{V}\tilde{\mathbf{S}}(i)}{\partial\boldsymbol{\theta}(i)}]^H[\frac{\partial\mathbf{V}\tilde{\mathbf{S}}(i)}{\partial vec(\mathbf{H})}]\\ &= -j\cdot diag\{\tilde{\mathbf{S}}^*(i)\}\mathbf{V}^H((\Theta(\varepsilon)(\mathbf{1}_{1\times N_T}\\ &\qquad\otimes\mathbf{F}^*)diag\{\tilde{\mathbf{S}}(i)\})\otimes\mathbf{I}_{N_R})\\ \Xi_i &= [\Xi_{1,i}, \Xi_{2,i}, j\Xi_{2,i}]\end{aligned} \tag{25}$$

and denote $\beta = [\varepsilon, Re\{vec(\mathbf{H})^T\}, Im\{vec(\mathbf{H})^T\}]^T$, the CRLB of β can be obtained as

$$\begin{aligned}\mathrm{CRLB}(\beta) = &\frac{2}{\sigma_z^2}[Re\{\Gamma\}\\ &-\sum_{i=1}^{N_S}Re\{\Xi_i^H\}Re\{diag\{\tilde{\mathbf{S}}^*(i)\}\mathbf{V}^H\mathbf{V}diag\{\tilde{\mathbf{S}}(i)\}\}^{-1}Re\{\Xi_i\}]^{-1}\end{aligned} \tag{26}$$

Then the first entry of $\mathrm{CRLB}(\beta)$ gives the CRLB for the CFO estimation $\mathrm{CRLB}(\varepsilon)$.

V. EXPERIMENTAL RESULTS

In this section, the efficiency of the proposed algorithm is examined in a two input two output MIMO-OFDM system with $N = 128$ subcarriers and the CP length is $L_{CP} = 16$. The channel has L independent Raleigh-fading taps with exponentially decaying powers set as $E[\left|h_{m,k}^{l}\right|^2] = e^{-l/3}/\sum_{i=0}^{L-1} e^{-i/3}, l = 0, 1, \ldots, L-1$. AWGN is added to each receiver with the signal to noise ratio (SNR) defined as $\mathrm{SNR} = 10\log_{10}\frac{\|x_m(i)-z_m(i)\|^2}{\|z_m(i)\|^2}$dB. The performance is evaluated by the bit error rate (BER) and mean square error (MSE) defined as $\mathrm{MSE} = \frac{1}{M_c}\sum_{p=1}^{M_c}\left|\varepsilon - \tilde{\varepsilon}_p\right|^2$, where $\tilde{\varepsilon}_p$ is the estimated value of ε in the p-th trial and the total number of Monte Carlo trials is $M_c = 1000$.

We first test the banded structure of the covariance matrices of the received signals under a six tap channel ($L = 6$) with QPSK transmitting signals. Let $V_\varepsilon(n) = \sum_{i=1}^{N_S}\sum_{m_1=1}^{N_R}\sum_{m_2=m_1}^{N_R}\left|r_{m_1,m_2,\varepsilon}^{n}(i)\right|^2, 0 \leq n \leq N-1$ denote the energy of the n-th element of the covariance vector of the received signals, Fig. 2 shows the curves of $V_\varepsilon(n)$ with 15dB SNR and $N_S = 7$ when there is no CFO ($\varepsilon = 0$), $\varepsilon = 0.3$ and the compensated result by the proposed estimator, respectively. Besides, the SISO case ($N_T = N_R = 1$) with $\varepsilon = 0$ is illustrated as a benchmark. It can be observed from Fig. 2 that $V_\varepsilon(n) \approx 0,\ L \leq n \leq N-L$ when $\varepsilon = 0$ in the SISO-OFDM system and the banded structure is weakened in the MIMO-OFDM system due to the interaction among different transmitting signals. However, the existence of CFO further weakens the banded structure and the CFO can be well estimated by the proposed algorithm.

In what follows, the estimation performance of the proposed algorithms is compared with the "Kurtosis", "PDE-F", "PDE-T", "Cov" and "Cov-fitting" algorithms, respectively. Since the algorithm of "Kurtosis" is also applied to non-constant modulus signals, the estimation performance of different algorithms for 16QAM transmitting signals are also established as comparisons. Unless otherwise specified, the normalized CFO is uniformly distributed in the range (−0.5,0.5) in all the simulations.

The resulting MSE and BER versus SNR with $N_S = 7$ under a six tap channel is demonstrated in Fig. 3 and Fig. 4, respectively. Besides, the CRLB performance is also shown in Fig. 3 as a comparison. The results verify the superior performance of the proposed algorithm over other algorithms and it can be observed that the proposed estimator is closer to CRLB, although all the algorithms suffer from an error floor under high-SNR regions. Furthermore, the algorithms all perform worse when the transmitting sources are 16QAM signals compared with the QPSK case, yet the proposed

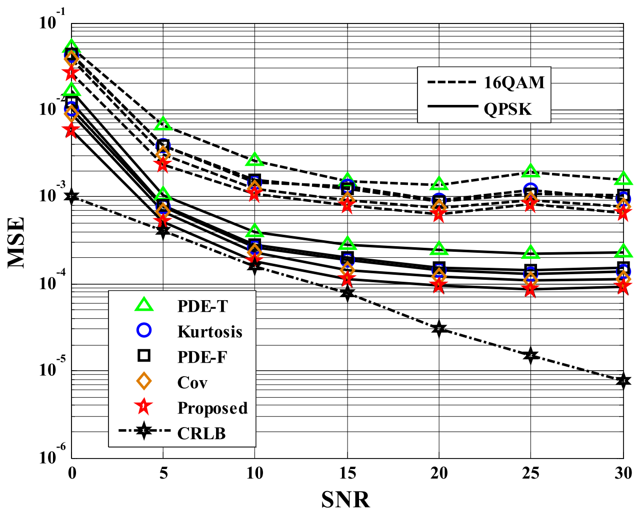

FIGURE 3. MSE versus SNR with $N_S = 7$ for QPSK and 16QAM transmitting signals, respectively.

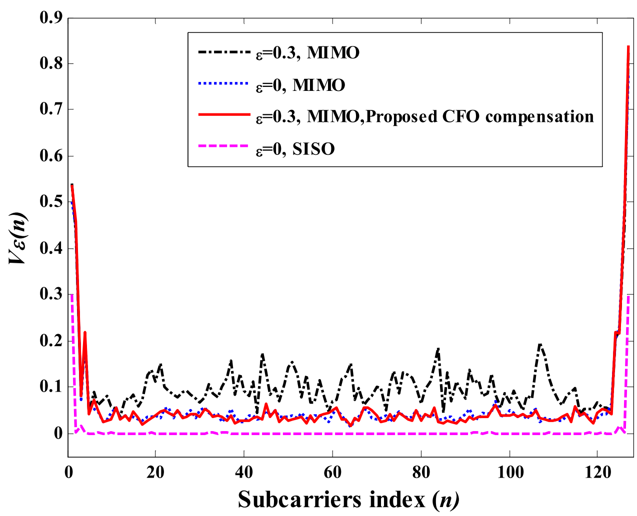

FIGURE 2. Curves of $V_\varepsilon(n)$ for QPSK transmitting symbols under a six tap channel.

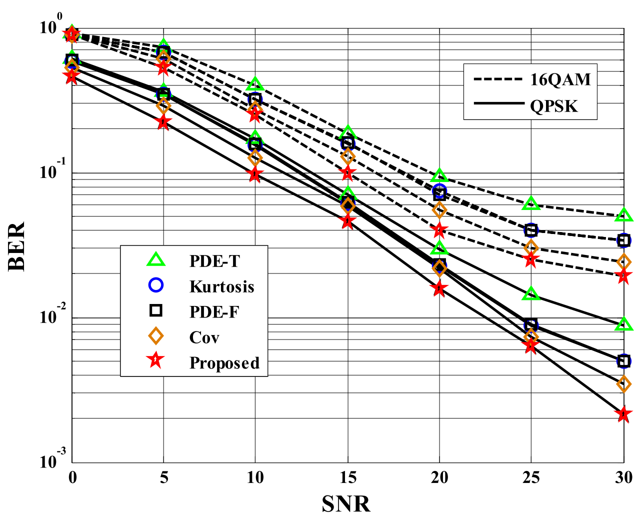

FIGURE 4. BER versus SNR with $N_S = 7$ for QPSK and 16QAM transmitting signals, respectively.

algorithm still outperforms other algorithms. Compared with the "Cov" algorithm, the performance of the proposed algorithm is improved. The reason is that the proposed algorithm utilizes the extra information in the cross-covariance of different received signals.

The MSE and BER versus block size N_S with 15dB SNR under a six tap channel is presented in Fig. 5 and Fig. 6, respectively. The CRLB curve is also plotted in Fig. 5. It can be observed that larger block size can improve the estimation performance, although the value of N_S is restricted by the coherence time of actual time-varying channels. The proposed algorithm, which almost reaches the CRLB, shows better performance than the other algorithms.

In order to evaluate the estimation performance of algorithms under different CFO values, Fig. 7 shows the MSE performance versus ε with 15dB SNR and $N_S = 7$ for QPSK transmitting signals. Apart from the superior performance of the proposed algorithm over other algorithms, it is seen that

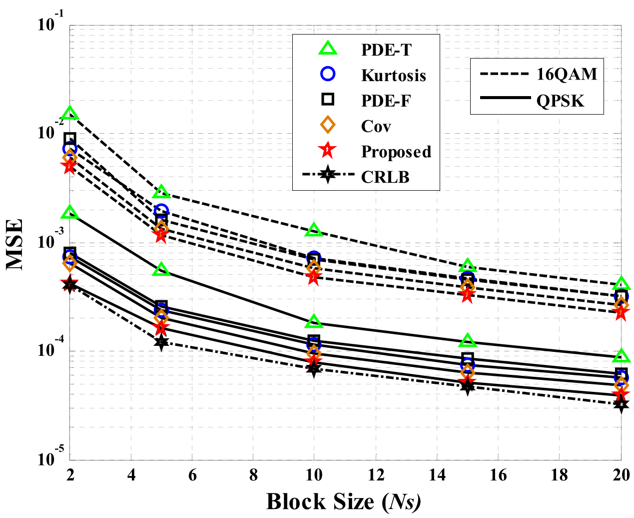

FIGURE 5. MSE versus N_S with 15dB SNR for QPSK and 16QAM transmitting signals, respectively.

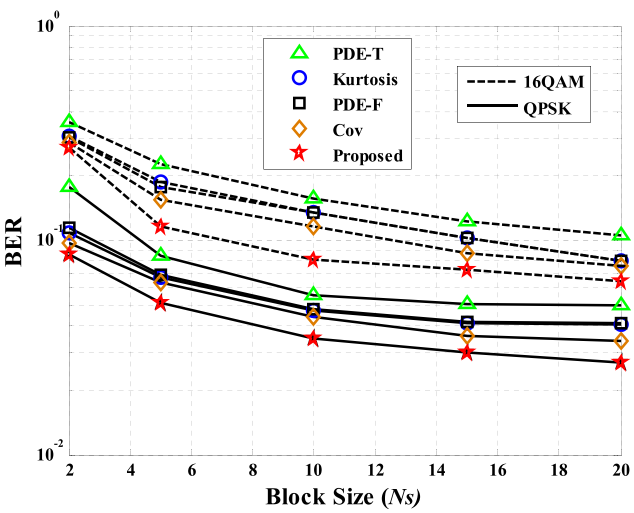

FIGURE 6. BER versus N_S with 15dB SNR for QPSK and 16QAM transmitting signals, respectively.

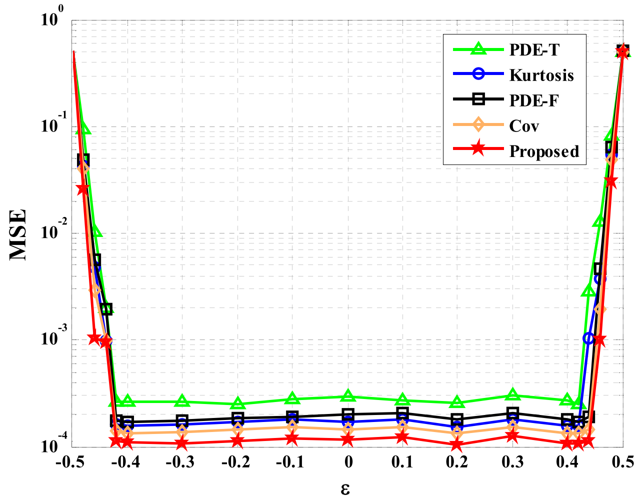

FIGURE 7. MSE versus ε with 15dB SNR and $N_S = 7$ for QPSK transmitting signals.

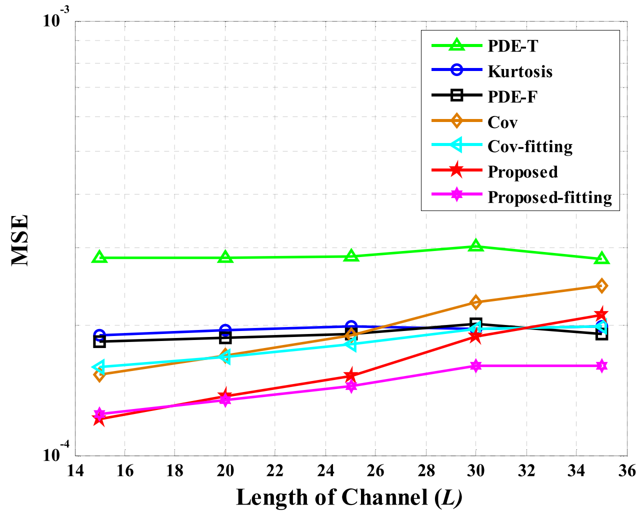

FIGURE 8. MSE versus L with 15dB SNR and $N_S = 7$ for QPSK transmitting signals.

performance of the algorithms remains basically unchanged unless $|\varepsilon|$ is very close to 0.5. This is not unexpected and the performance loss in large CFO can be compensated by means of null subcarriers [19].

To investigate the impact of channel length on the estimation performance, channels with increased lengths are generated along with the increase of CP length. Fig. 8 and Fig. 9 depict the MSE and BER versus L, respectively, with 15dB SNR and $N_S = 7$ for QPSK transmitting signals. As indicated by the results in Fig. 8 and Fig. 9, the "Kurtosis", "PDE-T" and "PDE-F" algorithms are almost invariant to channel length, while algorithms based on the banded structure of covariance matrices are affected by the channel length, just like the "Cov", "Cov-fitting", "Proposed" and "Proposed-fitting" methods. When the channel length gets longer, the out-of-band elements are less in number, which makes the proposed method perform worse. While for the "Proposed-fitting" algorithm, the incorporation of the

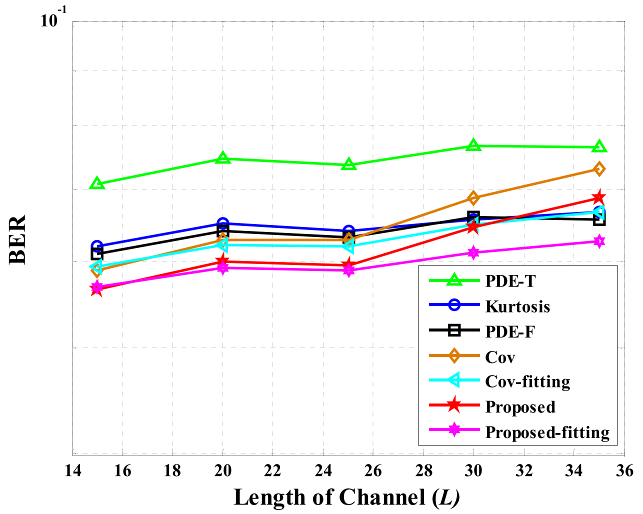

FIGURE 9. BER versus L with 15dB SNR and $N_S = 7$ for QPSK transmitting signals.

in-band elements amounts to lengthen the useful data, thus improving the estimation performance compared with the proposed one.

VI. CONCLUSIONS

In this paper, a blind CFO estimation algorithm is proposed for MIMO-OFDM systems. Observing that the banded structure of covariance matrices maintains in MIMO systems in the absence of CFO, a cost function is constructed by minimizing the out-of-band elements of the covariance matrices formed by circular shifts of received signals. Simulation results demonstrate the validity of the proposed algorithm under multipath frequency-selective channels. Furthermore, an improved algorithm is further developed by incorporating both the in-band and out-of-band information of covariance matrices, thus the performance degradation of the proposed algorithm can be alleviated when the channel length becomes longer. Since the proposed cost functions can be approximated by a sinusoidal closed form function, CFO can be easily estimated by a three-trial curve fitting method with low complexity.

APPENDIX A

The derivation of (14) is presented in this Appendix. First, (4) is re-written here as

$$\mathbf{y}_{m,\hat{\varepsilon}}(i) = \varphi^{(\varepsilon-\hat{\varepsilon})}(i)\sum_{k=1}^{N_T}\Theta(\varepsilon-\hat{\varepsilon})\mathbf{d}_{m,k}(i), \quad m = 1, 2, \ldots, N_R \tag{27}$$

where $\mathbf{d}_{m,k}(i) = \Phi_{m,k}\mathbf{F}^H\mathbf{S}_k(i)$ and the noise term is omitted for brevity. If $\mathbf{d}_{m,k}(i) = [d^0_{m,k}(i), d^1_{m,k}(i), \ldots, d^{N-1}_{m,k}(i)]^T$, the n-th element of $\mathbf{y}_{m,\hat{\varepsilon}}(i)$ is given by

$$y^n_{m,\hat{\varepsilon}}(i) = \varphi^{(\varepsilon-\hat{\varepsilon})}(i)e^{j\frac{2\pi(\varepsilon-\hat{\varepsilon})n}{N}}\sum_{k=1}^{N_T}d^n_{m,k}(i) \tag{28}$$

From (5) and (12), the n-th element of $\mathbf{r}_{m_1,m_2,\hat{\varepsilon}}(i)$ is

$$\begin{aligned} r^n_{m_1,m_2,\hat{\varepsilon}}(i) = &\sum_{p=0}^{N-n-1} y^{p+n}_{m_1,\hat{\varepsilon}}(i)\cdot {y^p_{m_2,\hat{\varepsilon}}}^*(i) \\ &+ \sum_{p=N-n}^{N-1} y^{p+n-N}_{m_1,\hat{\varepsilon}}(i)\cdot {y^p_{m_2,\hat{\varepsilon}}}^*(i), \quad 1\le n\le N-1 \end{aligned} \tag{29}$$

Submitting (28) into (29), there is

$$\begin{aligned} r^n_{m_1,m_2,\hat{\varepsilon}}(i) = &\, e^{j\frac{2\pi(\varepsilon-\hat{\varepsilon})n}{N}}\sum_{p=0}^{N-n-1}\sum_{k=1}^{N_T}d^{p+n}_{m_1,k}(i)\cdot\sum_{k=1}^{N_T}{d^p_{m_2,k}}^*(i) \\ &+ e^{j\frac{2\pi(\varepsilon-\hat{\varepsilon})(n-N)}{N}}\sum_{p=N-n}^{N-1}\sum_{k=1}^{N_T}d^{p+n-N}_{m_1,k}(i) \\ &\cdot\sum_{k=1}^{N_T}{d^p_{m_2,k}}^*(i) \end{aligned} \tag{30}$$

Let $\sum_{p=0}^{N-n-1}\sum_{k=1}^{N_T}d^{p+n}_{m_1,k}(i)\cdot\sum_{k=1}^{N_T}{d^p_{m_2,k}}^*(i) = \lambda^n_{m_1,m_2}(i)$ and $\sum_{p=N-n}^{N-1}\sum_{k=1}^{N_T}d^{p+n-N}_{m_1,k}(i)\cdot\sum_{k=1}^{N_T}{d^p_{m_2,k}}^*(i) = \mu^n_{m_1,m_2}(i)$, then there is

$$r^n_{m_1,m_2,\hat{\varepsilon}}(i) = e^{j\frac{2\pi(\varepsilon-\hat{\varepsilon})n}{N}}(\lambda^n_{m_1,m_2}(i) + e^{-j2\pi(\varepsilon-\hat{\varepsilon})}\mu^n_{m_1,m_2}(i)) \tag{31}$$

$$\begin{aligned} \left|r^n_{m_1,m_2,\hat{\varepsilon}}(i)\right|^2 = &\left|\lambda^n_{m_1,m_2}(i)\right|^2 + \left|\mu^n_{m_1,m_2}(i)\right|^2 \\ &+ 2Re\{\lambda^n_{m_1,m_2}(i)\mu^n_{m_1,m_2}(i)^*\}cos(2\pi(\varepsilon-\hat{\varepsilon})) \\ &- 2Im\{\lambda^n_{m_1,m_2}(i)\mu^n_{m_1,m_2}(i)^*\}sin(2\pi(\varepsilon-\hat{\varepsilon})) \end{aligned} \tag{32}$$

Since $r^n_{m_1,m_2}(i)$ for $L \le n \le N-L$ represents the out-of-band elements of $\mathbf{r}_{m_1,m_2}(i)$, $\lambda^n_{m_1,m_2}(i) + \mu^n_{m_1,m_2}(i)$ can be approximated as zero, thus $Im\{\lambda^n_{m_1,m_2}(i){\mu^n_{m_1,m_2}}^*(i)\} = -Im\{\left|\lambda^n_{m_1,m_2}(i)\right|^2\} \approx 0$ and $Re\{\lambda^n_{m_1,m_2}(i){\mu^n_{m_1,m_2}}^*(i)\} = -Re\{\left|\lambda^n_{m_1,m_2}(i)\right|^2\} < 0$. Therefore, (32) can be approximated as

$$\begin{aligned} \left|r^n_{m_1,m_2,\hat{\varepsilon}}(i)\right|^2 \approx &-2\left|\lambda^n_{m_1,m_2}(i)\right|^2 cos(2\pi(\varepsilon-\hat{\varepsilon})) \\ &+ 2\left|\lambda^n_{m_1,m_2}(i)\right|^2, \quad L\le n\le N-L \end{aligned} \tag{33}$$

and $J(\hat{\varepsilon}) \approx Acos(2\pi(\varepsilon-\hat{\varepsilon})) - A$ with $A < 0$ is proved straightforward.

APPENDIX B

The derivation of (18) is presented here. According to the results in Appendix **A**, $\left\|\mathbf{r}^Z_{m_1,m_2,\hat{\varepsilon}}(i+1)\right\|^2$ also follows (33).

$\mathbf{r}^{\mathrm{NZ}}_{m_1,m_2,\hat{\varepsilon}}(i+1)$ corresponds to the in-band elements and the a-th element of $\mathbf{r}^{\mathrm{NZ}}_{m_1,m_2,\hat{\varepsilon}}(i+1)$ can be written as

$$\begin{aligned} r^{a}_{m_1,m_2,\hat{\varepsilon}}(i+1) &= e^{j\frac{2\pi(\varepsilon-\hat{\varepsilon})a}{N}}(\lambda^{a}_{m_1,m_2}(i+1) \\ &\quad + e^{-j2\pi(\varepsilon-\hat{\varepsilon})}\mu^{a}_{m_1,m_2}(i+1)), \\ &a = 0,1,\ldots,L-1, \quad N-L+1,\ldots,N-1 \end{aligned} \tag{34}$$

Then there is

$$\begin{aligned} & r^{a}_{m_1,m_2,\hat{\varepsilon}}(i+1) - r^{a}_{m_1,m_2,\hat{\varepsilon}}(i) \\ &= e^{j\frac{2\pi(\varepsilon-\hat{\varepsilon})a}{N}}((\lambda^{a}_{m_1,m_2}(i+1) - \lambda^{a}_{m_1,m_2}(i)) \\ &\quad + e^{-j2\pi(\varepsilon-\hat{\varepsilon})}(\mu^{a}_{m_1,m_2}(i+1) - \mu^{a}_{m_1,m_2}(i))) \end{aligned} \tag{35}$$

Let $\lambda^{a}_{m_1,m_2}(i+1) - \lambda^{a}_{m_1,m_2}(i) = \lambda^{a}$ and $\mu^{a}_{m_1,m_2}(i+1) - \mu^{a}_{m_1,m_2}(i) = \mu^{a}$, then

$$\begin{aligned} & \left| r^{a}_{m_1,m_2,\hat{\varepsilon}}(i+1) - r^{a}_{m_1,m_2,\hat{\varepsilon}}(i) \right|^2 \\ &= \left|\lambda^{a}\right|^2 + \left|\mu^{a}\right|^2 + 2Re\{\lambda^{a}\mu^{a*}\}cos(2\pi(\varepsilon-\hat{\varepsilon})) \\ &\quad - 2Im\{\lambda^{a}\mu^{a*}\}sin(2\pi(\varepsilon-\hat{\varepsilon})) \end{aligned} \tag{36}$$

Since the channel is assumed to remain constant between two consecutive OFDM symbols, in the absence of CFO, there is $r^{a}_{m_1,m_2}(i+1) \approx r^{a}_{m_1,m_2}(i)$. Hence $\lambda^{a}_{m_1,m_2}(i+1) + \mu^{a}_{m_1,m_2}(i+1) \approx \lambda^{a}_{m_1,m_2}(i) + \mu^{a}_{m_1,m_2}(i)$ and $\lambda^{a}_{m_1,m_2}(i+1) - \lambda^{a}_{m_1,m_2}(i) \approx -(\mu^{a}_{m_1,m_2}(i+1) - \mu^{a}_{m_1,m_2}(i))$, i. e. $\lambda^{a} \approx -\mu^{a}$. Therefore, (36) can be approximated as

$$\begin{aligned} & \left| r^{a}_{m_1,m_2,\hat{\varepsilon}}(i+1) - r^{a}_{m_1,m_2,\hat{\varepsilon}}(i) \right|^2 \\ &\approx -2\left|\lambda^{a}\right|^2 cos(2\pi(\varepsilon-\hat{\varepsilon})) + 2\left|\lambda^{a}\right|^2, \\ &a = 0,1,\ldots,L-1,\ N-L+1,\ldots,N-1 \end{aligned} \tag{37}$$

and $\left\| \mathbf{r}^{\mathrm{NZ}}_{m_1,m_2,\hat{\varepsilon}}(i+1) - \mathbf{r}^{\mathrm{NZ}}_{m_1,m_2,\hat{\varepsilon}}(i) \right\|^2$ can be approximated as $A'cos(2\pi(\varepsilon-\hat{\varepsilon})) - A'$. Since all the terms in (17) are cosine functions with different constants independent of $\varepsilon - \hat{\varepsilon}$, the sum of them is also a cosine function with the same minimum and (18) can be proved accordingly.

ACKNOWLEDGMENT

The authors would like to thank the anonymous reviewers and editors for their careful reading and helpful remarks.

REFERENCES

[1] Y. Li and G. L. Stber, *Orthogonal Frequency Division Multiplexing for Wireless Communications*. Boston, MA, USA: Springer, 2006.

[2] P. Demestichas *et al.*, "5G on the horizon: Key challenges for the radio-access network," *IEEE Veh. Technol. Mag.*, vol. 8, no. 3, pp. 47–53, Sep. 2013.

[3] Y. Zeng, A. R. Leyman, and T.-S. Ng, "Joint semiblind frequency offset and channel estimation for multiuser MIMO-OFDM uplink," *IEEE Trans. Commun.*, vol. 55, no. 12, pp. 2270–2278, Dec. 2007.

[4] W. Zhang, Q. Yin, and F. Gao, "Computationally efficient blind estimation of carrier frequency offset for MIMO-OFDM systems," *IEEE Trans. Wireless Commun.*, vol. 15, no. 11, pp. 7644–7656, Nov. 2016.

[5] T. Jiang and N. D. Sidiropoulos, "A direct blind receiver for SIMO and MIMO OFDM systems subject to unknown frequency offset and multipath," in *Proc. 4th IEEE Workshop Signal Process. Adv. Wireless Commun.*, Jun. 2003, pp. 358–362.

[6] Z. Luo, L. Zhu, and C. Li, "Vandermonde constrained tensor decomposition based blind carrier frequency synchronization for OFDM transmissions," *Wireless Pers. Commun.*, vol. 95, no. 3, pp. 3459–3475, 2017.

[7] Y. Yao and G. B. Giannakis, "Blind carrier frequency offset estimation in SISO, MIMO, and multiuser OFDM systems," *IEEE Trans. Commun.*, vol. 53, no. 1, pp. 173–183, Jan. 2005.

[8] L. Wu, X. D. Zhang, and P. S. Li, "A low-complexity blind carrier frequency offset estimator for MIMO-OFDM systems," *IEEE Signal Process. Lett.*, vol. 15, pp. 769–772, 2008.

[9] X. N. Zeng and A. Ghrayeb, "A blind carrier frequency offset estimation scheme for OFDM systems with constant modulus signaling," *IEEE Trans. Commun.*, vol. 56, no. 7, pp. 1032–1037, Jul. 2008.

[10] L. Wu, X. D. Zhang, P. S. Li, and Y.-T. Su, "A blind CFO estimator based on smoothing power spectrum for OFDM systems," *IEEE Trans. Commun.*, vol. 57, no. 7, pp. 1924–1927, Jul. 2009.

[11] A. Al-Dweik, A. Hazmi, S. Younis, B. Sharif, and C. Tsimenidis, "Carrier frequency offset estimation for OFDM systems over mobile radio channels," *IEEE Trans. Veh. Technol.*, vol. 59, no. 2, pp. 974–979, Feb. 2010.

[12] S. Lmai, A. Bourré, C. Laot, and S. Houcke, "An efficient blind estimation of carrier frequency offset in OFDM systems," *IEEE Trans. Veh. Technol.*, vol. 63, no. 4, pp. 1945–1950, May 2014.

[13] J.-H. Oh, J.-G. Kim, and J.-T. Lim, "Blind carrier frequency offset estimation for OFDM systems with constant modulus constellations," *IEEE Commun. Lett.*, vol. 15, no. 9, pp. 971–973, Sep. 2011.

[14] A. Jayaprakash and G. R. Reddy, "Robust blind carrier frequency offset estimation algorithm for OFDM systems," *Wireless Pers. Commun.*, vol. 94, no. 3, pp. 777–791, 2017.

[15] A. Jayaprakash and G. R. Reddy, "Covariance-fitting-based blind carrier frequency offset estimation method for OFDM systems," *IEEE Trans. Veh. Technol.*, vol. 65, no. 12, pp. 10101–10105, Dec. 2016.

[16] W. Zhang, F. Gao, S. Jin, and H. Lin, "Frequency synchronization for uplink massive MIMO systems," *IEEE Trans. Wireless Commun.*, vol. 17, no. 1, pp. 235–249, Jan. 2018.

[17] W. Zhang and Q. Yin, "Blind carrier frequency offset estimation for MIMO-OFDM with constant modulus constellations via rank reduction criterion," *IEEE Trans. Veh. Technol.*, vol. 65, no. 8, pp. 6809–6815, Aug. 2016.

[18] Y. S. Cho, J. Kim, W. Y. Yang, and C. G. Kang, *MIMO-OFDM Wireless Communications With MATLAB*. Hoboken, NJ, USA: Wiley, 2010.

[19] W. Zhang, Q. Yin, and W. Wang, "Blind closed-form carrier frequency offset estimation for OFDM with multi-antenna receiver," *IEEE Trans. Veh. Technol.*, vol. 64, no. 8, pp. 3850–3856, Aug. 2015.

LIU YANG received the B.S. and M.S. degrees from the College of Communications Engineering, PLA University of Science and Technology, Nanjing, China, in 2012 and 2015, respectively. She is currently pursuing the Ph.D. degree with the Graduate School, Army Engineering University of PLA. Her research interests include wireless communications and blind signal processing.

HANG ZHANG received the B.S. degree from the PLA University of Science and Technology, Nanjing, China in 1984, and the M.S. degree from Southeast University, Nanjing, in 1989. She is currently a Professor and also a Ph.D. Supervisor with the Army Engineering University of PLA. Her research interests include wireless communications, satellite communications, and signal processing in communications.

YANG CAI received the B.S. and Ph.D. degrees from the College of Communications Engineering, PLA University of Science and Technology (PLAUST), Nanjing, China, in 2012 and 2017, respectively. He is currently a Lecturer with the Department of Electric and Optical Engineering, Space Engineering University of PLA, Beijing, China. His research interests include wireless communications, MIMO antennas, and beamforming arrays.

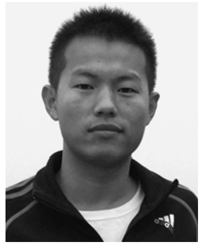

HUA YANG received the B.S. degree from the Beijing Institute of Technology, Beijing, China, in 2013, and the M.S. degree from the College of Communications Engineering, PLA University of Science and Technology, Nanjing, China, in 2016. He is currently pursuing the Ph.D. degree with the Graduate School, Army Engineering University of PLA. His research interests include wireless communications and blind signal processing.